

Assessment of Projectile Impact Initiation Hazards – A Review of Recent Experiments and Modelling

P J Haskins¹, M D Cook¹, A D Wood¹, R I Briggs¹, & P J Cheese²

¹*QinetiQ Ltd, Fort Halstead, Sevenoaks, Kent TN14 7BP, England*

²*Defence Ordnance Safety Group, Ash 2b #3212, MoD Abbey Wood, Bristol, BS34 8JH, England*

Abstract

In this presentation we will give the results of our most recent projectile impact experiments for two modern PBX materials, one cast and one pressed. This work has been carried out to characterise the SDT threshold for these materials when covered by varying barrier materials and thicknesses, and for a range of projectile shapes (including the approved STANAG projectile). We show how this work is directly applicable to the assessment of weapon hazards, and also provides data for the calibration and validation of reactive flow models. We compare these results with the predictions from our reactive flow model (CHARM) and outline our plans for future development of the model.

In addition, we describe some recent experiments designed to investigate XDT phenomena under projectile impact. In these experiments, the initial impact has been below the SDT threshold, but the damaged explosive has been allowed to expand and undergo a secondary impact with a rigid surface (either inert or energetic). We have observed XDT events in these experiments with melt-cast, cast-PBX, and pressed-PBX explosives. We discuss the possible implications of these findings for the hazard assessment of systems such as rocket motors and shaped charge warheads. Our work in this area is on-going and aimed at determining the precise conditions required for such XDT events with the ultimate hope of developing an understanding of the mechanism and a predictive capability.

Introduction

The response of explosives to fragment impact is of major importance to a weapon system's overall response to hazard. Fragments may be the primary cause of munition reaction when generated by a threat weapon. Alternately, fragments produced by violent reaction of munitions subjected to other hazards, such as spigot intrusion or fuel fire, can play a dominant role in the propagation of reaction, leading to sympathetic reaction and mass detonation. Knowledge of the response of energetic materials to fragment attack is therefore essential for munition design, application of mitigation techniques and overall safety assessment.

We have carried out many investigations into the effects of fragment impact on explosives during recent years^{1,2,3}, and the shock to detonation transition (SDT) threshold velocity has been determined for a number of septum material/projectile combinations. A predictive capability, based on the Cook-Haskins-Arrhenius Reaction Model (CHARM) has also been developed for the SDT response. The work described here builds on the results of previous studies and is part of an overall strategy to form a comprehensive database of experimental results and an associated modelling capability which can be used to assess the vulnerability of current and future weapon systems to fragment attack.

Experimental

Charge Preparation

The results for two explosives will be described in this paper; namely ROWANEX 1400 and ROWANEX 3000. ROWANEX 1400 is a cast PBX consisting of 66% RDX, 22% aluminium and 12% HTPB binder. The second explosive, ROWANEX 3000, is a high performance pressed PBX with 95%HMX and 5% HTPB as a binder. Both compositions were manufactured by BAe Systems Land Systems. The charges were 50mm in diameter and 50mm in length with average densities of 1.784g/cc and 1.692g/cc for ROWANEX 1400 and 3000 respectively.

Projectiles

Flat-ended cylindrical steel projectiles were used in two diameters: 13.15mm and 20mm. The 13.15mm projectiles were 25.4 mm long. The 20mm diameter projectiles were somewhat shorter so as to be of equal mass (27g) to the 13.15mm projectile. Additionally, some 13.15mm diameter projectiles with various conical tips were used in the XDT studies. Further experiments were also carried out using the new STANAG 4496 fragment, which is a 14.30mm right regular cylinder with a conical tip of included angle 160°.

The projectiles were sub-calibre, and as a result were housed in nylon sabots before firing from a 30mm RARDEN gun. The projectiles were propelled using a standard 30mm RARDEN percussion cartridge filled with a known quantity of NRN41 propellant. The precise quantity of propellant in the cartridge was varied from round to round to produce fragment velocities up to ca. 2100 m/s.

Experimental Set-up

The explosive targets were placed on wooden blocks and carefully taped to a steel support beam so that the axis of the cylindrical explosive charge was aligned with the path of the projectile. The steel support beam was attached to a sabot stripping plate to provide proper alignment of the target with the path of the projectile. Two marker bars were attached to the support beam a known distance (0.5m) apart to permit the later determination of scale from the film record. The projectiles were fired at the target through a 50mm

diameter hole in the sabot stripping plate to guarantee that only the projectile made contact with the target. A bank of flash bulbs and a diffusing screen illuminated the experiment and these were synchronised with the firing of the gun to enable photography of the last half metre of projectile travel, and the target response.

Instrumentation

Firings were observed with a Photonics Phantom 7 digital video camera. A range of framing rates was used in this work from 47000 to 160,000fps. Two banks of seven flash bulbs were used to back-illuminate the store. The video record was used to determine projectile velocities, reveal projectile orientation at the moment of impact, and provide visual confirmation of the degree of reaction of the target store. Projectile velocities are estimated to be accurate to ca. $\pm 5\%$.

Sequence of Firings

Septum thickness and projectile velocity were varied to determine the threshold impact velocity for SDT at each barrier/projectile combination. In addition, some effort was made to attempt to discriminate lesser degrees of reaction, although these are not discussed here. For studies of XDT phenomena a variety of charge configurations have been studied and these are described later.

Results

Figure 1 is a summary of all the experimental results for ROWANEX 3000. This includes tests through both aluminium and steel barriers and with three types of projectile. These figures show the fastest projectile velocity that produced a non-detonative response in the target, and the slowest projectile velocity that produced a prompt detonation in the target.

It is clear from this plot that the following general trends apply:

- The projectile threshold velocity required to induce a detonation in the target generally increases as the barrier plate thickness increases.
- The SDT threshold velocity is higher for conical tipped projectiles (e.g. the STANAG 4496 projectile used here) than for flat-ended projectiles of the same, or comparable, diameter.
- For a given barrier thickness steel barriers result in higher threshold velocities than aluminium barriers.
- For a given barrier material and thickness the projectile threshold velocity required to produce a detonation decreases with increasing projectile diameter for flat faced projectiles.

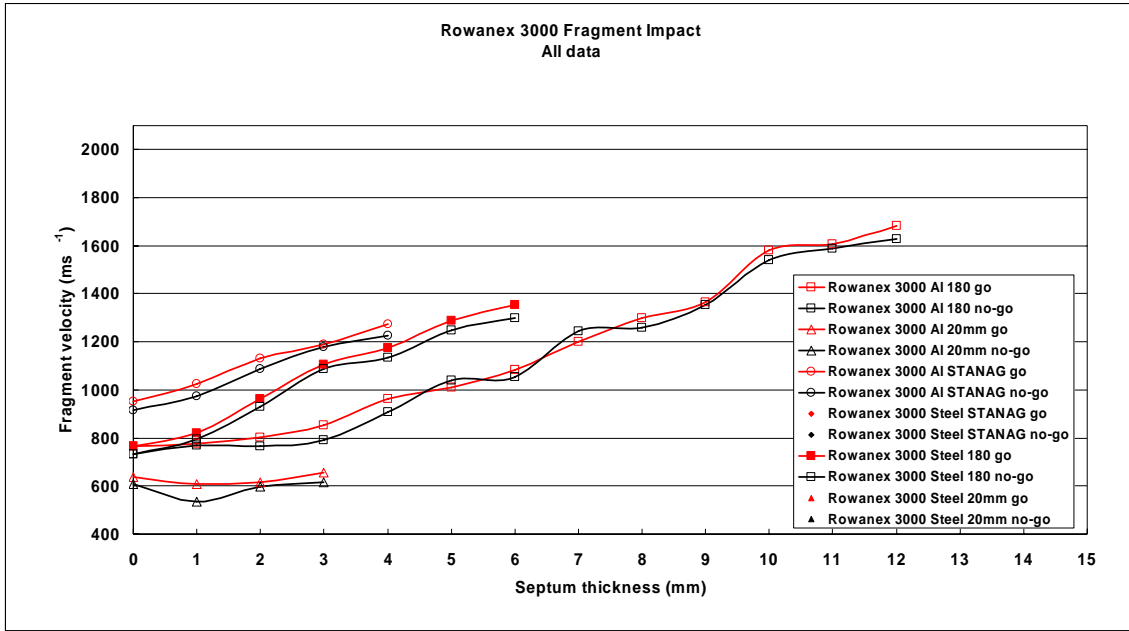


Figure 1. Experimental data for ROWANEX 3000 firings employing 13.15mm, 20mm and STANAG 4496 (14.3mm diameter) projectiles through both aluminium and steel barriers.

In Figure 2 we show the experimental SDT threshold data for ROWANEX 1400 with aluminium cover plates and 13.15mm flat-ended projectiles. We also show the CHARM fit to this data.

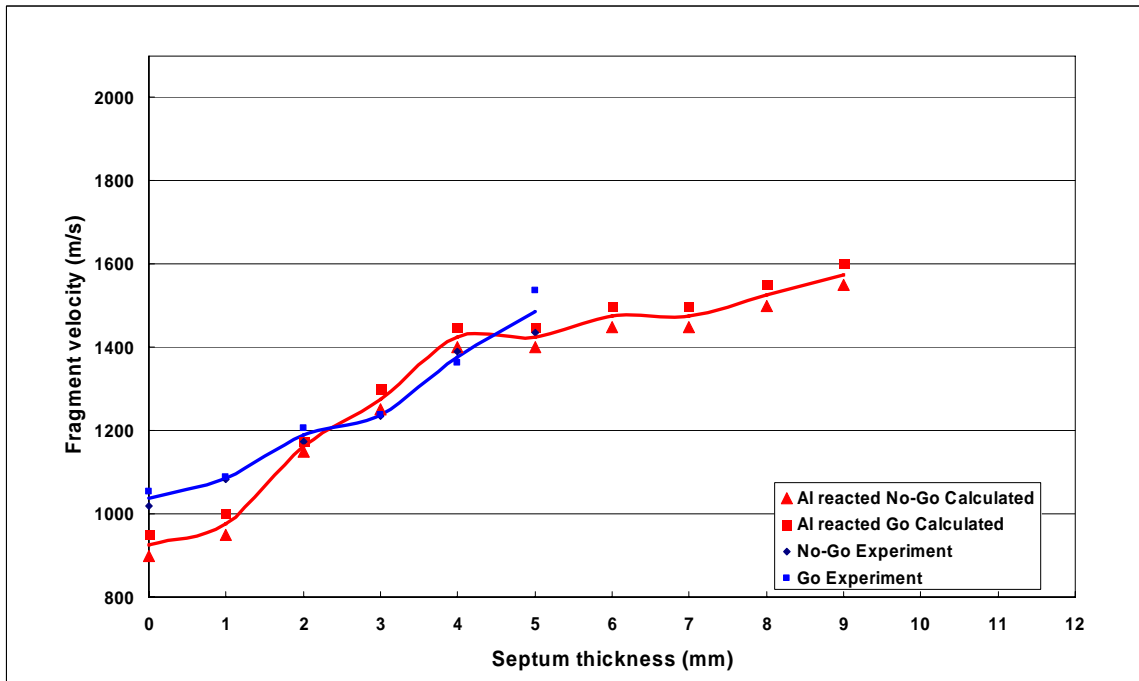


Figure 2. Plot of the response for ROWANEX 1400 with aluminium cover plates attacked by 13.15mm projectiles. The experimental data is shown in blue and the predicted values, using CHARM, are given in red.

Comparison of Figures 1 and 2 shows, not surprisingly, that ROWANEX 3000 is significantly more sensitive than ROWANEX 1400. For ROWANEX 3000 covered by steel barriers and for the STANAG 4496 projectile with aluminium barriers there is a relatively linear increase in SDT threshold velocity with barrier thickness, and any structure present in this curve is almost certainly obscured by experimental errors. However, the ROWANEX 3000 data for the two diameters of flat-ended projectile through aluminium cover plates show a distinctly flat response out to barrier thicknesses of 3mm (or possibly more for the 20mm projectile, as this region has not been explored).

Reactive Modelling

Modelling of munitions is becoming increasingly important both from the vulnerability as well as the performance point of view. One key part of any model is the ability to describe the behaviour of the energetic components. Such models are usually referred to as ignition and growth of reaction models.

Traditional models used to describe the ignition and growth of reaction in explosives are generally based on a pressure dependent reaction rate law. The CHARM model used to model explosive response in this work has been developed over a number of years. It is set apart from other ignition and growth of reaction models in that it is temperature dependent and uses three-step Arrhenius chemistry to describe the chemical reaction from solid (or liquid or gaseous) explosive to gaseous products with the associated release of energy.

The basic CHARM model⁴ can be used to model homogeneous explosives. A further feature of this model is that it has a number of explicit hot spot models (based on gas pore collapse, cumulative damage and friction/shear) that act with the underlying homogeneous model to reproduce heterogeneous features such as shock desensitisation. Thus CHARM has the capability to describe both homogeneous and heterogeneous behaviour, and features such as shock desensitisation, in a physically meaningful way.

The model comprises of an unreacted equation of state which describes how energy is dissipated into the energetic material under shock impact, a reacted equation of state that describes how the gaseous products do work on the environment, and a coupled three-step Arrhenius reaction scheme that controls the chemistry and the release of energy. Each of the Arrhenius reaction steps is associated with a reaction energy, which may be endothermic or exothermic. The rate of reaction of each step is a function of the Arrhenius parameters, the concentrations of the constituents, the temperature and (optionally) the pressure. The overall reaction scheme releases energy, which fuels the decomposition. If the energy release rate is sufficiently fast the burn will run-away to detonation. The model is implemented in the Lagrange, non-linear, explicit, two-dimensional finite element code, DYNA2D and the Eulerian hydrocode GRIM as an equation of state.

There are a number of parameters that are required by CHARM but most are standard physical constants. Under shock conditions, the behaviour can be described by an unreacted equation of state. This typically takes the form of a shock velocity – particle velocity relationship. These data are available for a wide range of materials and are generally obtained from gas gun experiments.

The product gases, formed once the explosive has reacted, are described by their own equation of state. The one most commonly used is the Jones-Wilkins-Lee (JWL) equation of state (EOS) and this is used in CHARM to describe the pressure – volume – energy behaviour of the detonation products. The JWL parameters are usually fitted to experimental data from cylinder tests, but if these are unavailable a JWL EOS can be calculated using a thermochemical equilibrium code such as Cheetah⁵. CHARM also has a table look-up feature which can be populated to describe both the unreacted explosive and product gases.

The three-step Arrhenius chemistry parameters used in the CHARM model can be obtained by calibrating the same Arrhenius chemistry scheme within a finite element heat flow code to fit small-scale confined heating experiments on the energetic material . The parameters so obtained can be used directly in the CHARM model. Hot spot parameters are either obtained from the literature (as is the case for the thermal conductivity and heat capacity of the energetic material), or tuned to flyer plate and/or projectile impact data.

Predictions for ROWANEX 1400

To date modelling has only been carried out for the experiments on ROWANEX 1400. It can be seen from figure 2 that a good fit to the experimental data has been achieved for the 13.15mm diameter flat-ended projectile data with aluminium barriers. This gives confidence in both the CHARM model and the parameterisation for ROWANEX 1400. Data is currently being gathered for this explosive with other projectiles and with steel barriers. The model should thus prove extremely useful in assessing the fragment impact vulnerability of a weapon system containing this PBX.

XDT

In recent years we have carried out several hundred projectile impact experiments to investigate XDT processes. These have included all types of explosive formulation (melt cast, cast PBX, mouldable demolition explosive, and pressed PBX) and all have been shown susceptible to this phenomenon. Here we summarise only our most recent experiments on ROWANEX 3000. The experiments were designed so that the shocks generated on projectile impact were below the threshold conditions for SDT. However, the charges were positioned such that after projectile strike the expanding explosive material would impact a rigid surface placed a short distance away.

A total of 17 tests have been carried out to date in an effort to study XDT in ROWANEX 3000. For these tests the charges consisted of 50mm x 50mm

cylinders of average density 1.692 g/cc, as for the SDT experiments. A number of different arrangements were used for these tests, although all involved two explosive charges (to represent a charge cavity). In a number of the tests the front charge (which was impacted by the projectile) was bare and a second charge was placed behind at a distance of 12.7, 25.4 or 50.8mm. Using 150° conical-tipped projectiles XDT was observed when the gap was 25.4mm, but not at 12.7 or 50.8mm. A similar result was obtained when the front charge was covered with a 3mm steel barrier plate (See Figure 3). XDT events were also obtained in tests involving a more complex arrangement consisting of steel front cover plate (both 3 and 5mm were used), front charge backed by 1mm aluminium, an air gap, and a second charge covered with a 1mm aluminium plate. Using 120° conical-tipped projectiles XDT was again observed when the gap was 25.4mm. This arrangement was chosen to be analogous to the situation in the cone region of a shaped charge warhead. Consequently, this result suggests a potential XDT hazard for weapons of this kind.



Figure 3. Experimental Set-Up for an XDT experiment with 2 ROWANEX 3000 charges and a steel cover plate.

These latest XDT experiments, taken with our earlier results on other compositions, have led us to the hypothesis that the XDT mechanism operating under projectile impact conditions can be considered a two-stage process. The first stage is the creation of damaged, more sensitive, energetic material, and the second is initiation of the damaged material by re-shock/re-compression. For this mechanism to operate it is clear that we require the following conditions:

- A sufficiently fast impact (but below the SDT threshold conditions) to create rapidly moving damaged material.
- A space into which the damaged material can accelerate.
- A secondary surface to create re-shock/re-compression.

Conclusions and Way Forward

The experimental data generated by the kind of experiment described here is invaluable both for direct empirical assessment of hazards, and also for the calibration and validation of models such as CHARM. Because of interest in thick-cased munitions and/or insensitive explosives there is a requirement to extend the study of SDT thresholds to higher velocities. As a consequence we are currently testing a new 40mm gun system which will enable velocities of ca. 2500m/s to be achieved.

We have shown that the current CHARM model is able to reproduce the prompt SDT characteristics of a modern PBX with reasonable accuracy. Nevertheless, we are currently implementing improvements to the CHARM model, most notably to incorporate a grain burning functionality. It is hoped that this will not only lead to more accurate modelling of SDT phenomena, but also provide a predictive capability with regard to particle size effects in compositions. In the longer term we also hope to build on this framework for the modelling of non-SDT responses.

The qualitative understanding of the XDT process which has arisen from this work should be of help in irradiating the problem from future system designs. However, further progress will be dependent on the development of a quantitative modelling capability. This is a difficult task as it requires both a model for the material properties of the explosive at high rates of strain, and a model for the shock sensitivity of the damaged material.

References

1. M. D. Cook, P. J. Haskins, "Projectile Initiation of Explosive Charges", 9th Symposium (International) on Detonation, Portland OR, 1989, Vol II, OCNR113291-7, p1441.
2. M. D. Cook, P. J. Haskins, R. I. Briggs, C. Stennett, J. Fellows, "High-speed observation of fragment impact initiation of nitromethane charges", 11th APS Topical Group on Shock Compression of Condensed Matter, Snowbird, UT, 1999, ISSN0094-243X, Vol II, p793.
3. M. D. Cook, P. J. Haskins, R. I. Briggs, C. Stennett, J. Fellows, and P. J. Cheese, "Fragment Impact Characteristics of Melt-cast and PBX Explosives", Proceedings of the Conference of the APS Topical Group on Shock Compression of Condensed Matter, Atlanta, Georgia, June 24-29, 2001.
4. M. D. Cook, P. J. Haskins and C. Stennett, "Development and Implementation of an Ignition and Growth Model for Homogeneous and

- Heterogeneous Explosives", Proceedings of the Eleventh Symposium (International) on Detonation, Snowmass, Colorado, 30 August-4 September 1998, p587.
5. "CHEETAH Ideal Detonation Code", L E Fried, LLNL, UCRL-MA-117541.

© QinetiQ Ltd, 2006.